Solvation of SCN^- and $SeCN^-$ Anions in Hydrogen-Bonding Solvents

Philip W. Schultz, George E. Leroi,* and Alexander I. Popov*

Contribution from the Department of Chemistry, Michigan State University, East Lansing, Michigan 48824-1322

Received March 18, 1996[⊗]

Abstract: The primary solvation sphere surrounding the thiocyanate or the selenocyanide anion in protic solvents, such as methanol, *N*-methylformamide and formamide, forms intimate hydrogen bonds with these anions. These interactions perturb the electron density and vibrational modes of these anions and can therefore be studied by NMR and infrared spectroscopies. In neat solutions, these solvents form hydrogen bonds to the nitrogen end along the molecular axis and nonaxially to the π cloud of the C−N bond, although a substantial proportion of the anions is not hydrogen bonded. In nitromethane solutions, the thiocyanate and selenocyanide anions form weak complexes with methanol and the amide solvents ($K < 1\ M^{-1}$), which is an order of magnitude smaller than that of OCN^- with the same solvents, determined in our previous investigation of the cyanate anion. The remarkable differences in the solvation of these singly charged anions can be understood by theoretical calculations of their electrostatic potentials.

Introduction

Electrolyte solutions and the equilibria that exist in them have been of long-standing interest in chemistry. Many types of interactions may occur in an electrolyte solution; their strength varies from weak van der Waals forces to strong electrostatic attractions. This wide range of attractive forces and the abundance of interaction sites result in a large number of solution equilibria that are difficult to sort out experimentally.[1] The types of interactions can be broadly categorized as solvent−solvent, ion−solvent, and ion−ion. The relative importance of the resulting equilibria depends upon the nature of the electrolyte and of the solvent.

The thiocyanate and selenocyanide anions have been used as spectroscopic probes of ionic association in alkali and alkaline earth metal complexes in solution because the stretching modes for these anions are easily observed and are sensitive to electrostatic interactions.[2−10] Both the SCN^- and $SeCN^-$ anions have three fundamental vibrations, all of which are infrared active. The highest frequency mode (ν_3), which is commonly labeled the ν_{CN} stretch, occurs at 2058 cm^{-1} for SCN^- and 2066 cm^{-1} for $SeCN^-$ in DMSO.[11−13] The lowest frequency mode (ν_2), which occurs at ∼465 cm^{-1} for SCN^- and ∼450 cm^{-1} for $SeCN^-$, is the doubly degenerate bending vibration, labeled δ_{SCN} and δ_{SeCN}, respectively.[11−13] The second stretching vibration (ν_1) occurs at 735 cm^{-1} for SCN^- in DMF solutions, and is commonly termed ν_{CS}.[11−13] The comparable ν_{CSe} vibration for $SeCN^-$ is not observed experimentally and is predicted to have a very low dipole moment derivative,[14] although it can be seen in LiNCSe ion pairs.[13] The justification for these labels has been demonstrated by *ab initio* calculations, from which the potential energy distribution for the ν_{CN} modes of these anions was found to be about 90% C−N stretch.[14]

The perturbations of the stretching modes by electrostatic interactions have been studied by a number of authors.[2−10] From these investigations, the structures of numerous solution species have been correlated with their unique vibrational frequencies. In general, alkali and alkaline earth metal cations interact with the nitrogen atom of SCN^-, which raises the frequencies of both stretching modes with respect to the unperturbed anion. Similar results have been reported for the limited studies of $SeCN^-$ systems.[4] Interaction at the sulfur end of SCN^-, as exemplified by the Ag^+SCN^- ion pair, lowers the frequency of the ν_{CN} stretch and raises the frequency of the ν_{CS} mode relative to SCN^-.[15] In dimer systems, such as $(LiNCS)_2$ and $(LiNCSe)_2$, each anion is bridged by two lithium cations, which reduces the frequency of the ν_{CN} vibration and increases the frequencies of the ν_{CS} and ν_{CSe} modes.[4,6]

Likewise, hydrogen bonding interactions with these anions perturb the frequencies of the stretching modes, from which inferences about structures of the complexes that are formed can be drawn. Perelygin and Mikhailov observed that hydrogen bonding solvents shift the peak maximum and broaden the spectral envelope of the ν_{CN} stretch of SCN^- compared to the absorptions measured in aprotic solvents.[16] Corset and co-workers assigned a blue shift of the ν_{CN} mode, when phenol was added to a solution of tetrabutylammonium thiocyante (NBu_4SCN) in CCl_4, to the formation of a hydrogen bond at

[⊗] Abstract published in *Advance ACS Abstracts,* October 15, 1996.

(1) Barthel, J.; Gores, H.; Schmeer, G.; Wachter, R. *Top. Curr. Chem.* **1983**, *111*, 33.
(2) Irish, D. E.; Tang, S.-Y.; Talts, H.; Petrucci, S. *J. Phys. Chem.* **1979**, *83*, 3268.
(3) Perelygin, I. S.; Klimchuk, M. A. *Z. Struk. Khimi* **1983**, *24*, 67.
(4) Paoli, D.; Chabanel, M. *J. Chem. Res. (S)* **1991**, 360.
(5) Saar, D.; Petrucci, S. *J. Phys. Chem.* **1986**, *90*, 3326.
(6) Chabanel, M. *Pure Appl. Chem.* **1990**, *62*, 35.
(7) Chabanel, M.; Wang, Z. *J. Chem. Phys.* **1984**, *88*, 1441.
(8) Firman, P.; Xu, M.; Eyring, E.; Petrucci, S. *J. Phys. Chem.* **1992**, *96*, 8631.
(9) Mamantov, G.; Popov, A. I. *Chemistry of Nonaqueous Solutions: Current Progress*; VCH: New York, 1994; Chapter 2.
(10) Touaj, K.; Chabanel, M. *J. Chem. Soc., Faraday Trans.* **1995**, *91*, 4395.
(11) Colthup, N. B.; Daly, L. H.; Wiberley, S. E. *Introduction to Infrared and Raman Spectroscopy*; Academic Press, Inc.: Boston, 1990; p 239.
(12) Nakamoto, K. *IR and Raman Spectra of Inorganic and Coordination Compounds*; Wiley: New York, 1978.
(13) Golub, A. M.; Köhler, H. *Chemistry of Pseudohalides*, Elsevier: Amsterdam, 1986; Chapters 4−6.
(14) Schultz, P. W.; Leroi, G. E.; Harrison, J. F. *Mol. Phys.* **1996**, *88*, 217.
(15) Paoli, D.; Maryvonne, L.; Chabanel, M. *Spectrochim. Acta.* **1978**, *34A*, 1087.
(16) Perelygin, I.; Mikhailov, G. *Russ. J. Phys. Chem.* **1990**, *64*, 1060.

S0002-7863(96)00882-7 CCC: $12.00

the nitrogen atom of SCN^-.[17] Gill and co-workers measured the infrared spectrum of NBu_4SCN in MeOH and deconvolved the ν_{CN} spectral envelope into six component bands.[18] The 2054-cm^{-1} band, which has the largest absorptivity of all the components, was assigned to "free" SCN^-. Another study of SCN^- in methanol by Bencheikh showed that only four bands are necessary to simulate the ν_{CN} spectral envelope (2090, 2071, 2055, and 2037 cm^{-1}).[20] Recently, Hochstrasser and co-workers have studied the vibrational relaxation of SCN^- in D_2O and MeOH.[21,22] Their results are consistent with hydrogen bonding of the solvent to the nitrogen end of the thiocyanate anion. X-ray diffraction studies of NaSCN in methanol imply that two methanol molecules are hydrogen bonded to the nitrogen of SCN^-, with a bond angle of 120°.[23]

As the perturbations in the vibrational modes reveal, electrostatic interactions with SCN^- and $SeCN^-$ alter their electronic structure. All of the nuclei in the SCN^- and $SeCN^-$ anions have magnetically active isotopes,[24] and with the exception of ^{33}S, which has a large quadrupole moment, the shifts in electron density can be easily studied by multinuclear NMR spectroscopy. ^{15}N NMR spectroscopy has been employed to identify the isomers of organo-thiocyanates and isothiocyanates. RNCS compounds are characterized by a ^{15}N NMR shift of −275 ppm whereas RSCN compounds have a ^{15}N chemical shift of −100 ppm; both are large shifts from that of the free anion at −165 ppm.[25] Ionic associations of SCN^- with Li^+ have been studied by ^{15}N NMR spectroscopy, where interactions to either the sulfur or nitrogen atoms were identified by the paramagnetic or diamagnetic shifts, respectively.[26] Musikas et al. studied the binding of SCN^- to several lanthanide ions by the perturbations in the chemical shift and relaxation time of the nitrogen nuclei.[27] Similarly, the ^{77}Se chemical shifts for $SeCN^-$ are extremely sensitive to ionic interactions. In DMSO solutions, ionic interactions to the nitrogen atom increase the shielding from −273 ppm for $SeCN^-$ to −318 ppm for a zinc complex with $SeCN^-$. Interactions to the selenium end, exemplified by a mercury complex, decrease the shielding to −191 ppm.[28] In contrast to the large shifts observed for the nitrogen and chalcogen nuclei, the ^{13}C resonances in SCN^- and $SeCN^-$ are not very sensitive to bonding at either end of these anions.[29]

The quadrupolar relaxation of the ^{14}N resonance provides additional information about solution equilibria. Formation constants for several ionic complexes have been determined from the change in the line widths of quadrupolar nuclei.[30−33] In the case of SCN^- in H_2O, Au-Yeng found that the ^{14}N line width is sensitive to the ion−solvent interaction; the concentration dependence of the ^{14}N line width is consistent with the electron distortion model, which relates the distortion in the paramagnetic shielding contribution of the chemical shift to the relaxation rate of the resonance.[34]

Scheme 1. Ion Pair Formation Equilibrium

$$M^+(S_x) + SCN^-(S_y) \rightleftharpoons M^+NCS^-(S_n) + (x + y - n)S$$

Thermodynamic parameters for the formation of alkali metal thiocyanate ion pairs, dimers, and tetramers in several nonaqueous solvents have been derived by many investigators.[7−10] Despite the strong Coulombic attraction between the cation and anion, the important role of the solvent in ion pair formation equilibria makes the process, in general, entropy driven.[9] This is illustrated for the alkali thiocyanates in Scheme 1. The reduction in entropy resulting from the formation of the ion pair is more than balanced by an increase in entropy due to the release of solvent molecules from the separated solvated ions. Likewise, the negative enthalpy contribution from the Coulombic attraction of the cation and anion is balanced by the energy needed to break ion−solvent bonds in the solvated ions. Our previous investigation of cyanate−solvent complexes illustrated the role of entropy and the importance of solvent self association in the formation of anion−solvent complexes.[35]

Several solvent properties have been identified as indicators of the extent of ion pairing in an electrolyte solution namely the dielectric constant, the dipole moment, and the solvating ability of the solvent. The solvating ability is described by two empirical scales, the donor and the acceptor numbers.[36] Despite the importance of the nature of ionic solvation in ion pairing, the factors involved in ion−solvent interactions, especially anion-solvation, have not been thoroughly studied. From the perspective of the anion, the solvent in an electrolyte solution can be divided into three regions: the primary solvation shell surrounding the ion, the secondary solvation shell, and the bulk liquid.[37] Solvent molecules that are in closest and intimate contact with an ion belong to the primary solvation shell. The ion's charge provides an electrostatic attraction that brings the solvent closer than the sum of the respective van der Waals radii.[37] In the secondary solvation shell, the solvent molecules are attracted to the ionic charge, while not in intimate contact with the ion. The bulk liquid is free of any significant electrostatic effect from the anion.

In this paper, we address the structure of the primary solvation shell surrounding the thiocyanate and selenocyanide anions in nonaqueous protic solvents. The protic solvents used in this investigation are methanol (MeOH), formamide (FA), and *N*-methylformamide (NMF); this series allows a variety of hydrogen bonding interactions to be studied. NMR and infrared spectroscopies are employed to probe the interactions in these solutions and provide data from which the thermodynamics of the equilibria which exist in them can be calculated. Spectroscopic measurements are reported for the thiocyanate and selenocyanide anions both in neat solutions of the appropriate salt and protic solvents, and in an "inert" solvent where the

(17) Bacelon, P.; Corset, J.; de Loze, C. *J. Solution Chem.* **1983**, *12*, 13.
(18) Bachelin, M.; Gans, P.; Gill, J. B. *J. Chem. Soc., Faraday Trans.* **1992**, *88*, 3327.
(19) Kuhn, L. P.; Bowman, R. E. *Spectrochim. Acta, Part A* **1967**, *23*, 189.
(20) Bencheikh, A. Thèse 3° cycle, Nantes, 1987.
(21) Owrutsky, J.; Raftery, D.; Hochstrasser, R. M. *Annu. Rev. Chem.* **1994**, *45*, 519.
(22) Owrutshky, M.; Sarisky, M.; Culver, J.; Yodh, A.; Hochstrasser, R. M. *J. Chem. Phys.* **1993**, *98*, 5499.
(23) Kameda, Y.; Takahashi, R.; Usuki, T.; Uemura, O. *Bull. Chem. Soc. Jpn.* **1994**, *67*, 956.
(24) Mason, J. *Multinuclear NMR*; Plenum: New York, 1985.
(25) Giffard, M.; Cousseau, J.; Martin, G. J. *J. Chem. Soc., Perkin Trans. 2* **1985**, 157.
(26) Vaes, J.; Chabanel, M.; Martin, M. L. *J. Phys. Chem.* **1978**, *82*, 2420.
(27) Musikas, C., Cuillerdier, C.; Chachaty, C. *Inorg. Chem.* **1978**, *17*, 3610.
(28) Pan, W-H.; Fackler, J. P.; Kargol, J. A.; Burmeister, J. L. *Inorg. Chim. Acta* **1980**, *44*, L95.
(29) Kargol, J. A.; Crecely, R. W.; Burmeister, J. L. *Inorg. Chem.* **1979**, *18*, 2532.
(30) Nicholas, A. M.; Wasylishen, R. E. *Can. J. Chem.* **1987**, *65*, 951.
(31) Owens, G.; Guarilloff, P.; Steel, B. J.; Kurucsev, T. *Aust. J. Chem.* **1995**, *48*, 207.
(32) Berman, H. A.; Stengle, T. R. *J. Phys. Chem.* **1975**, *79*, 1001.
(33) Miller, A. G.; Franz, J. A.; Macklin, J. W. *J. Phys. Chem.* **1985**, *89*, 1190.
(34) Au-Yeung, S. C. *J. Magn. Reson.* **1991**, *92*, 10.
(35) Schultz, P. W.; Leroi, G. E.; Popov, A. I. *J. Am. Chem. Soc.* **1995**, *117*, 10735.
(36) Gutmann, V. *The Donor−Acceptor Approach to Molecular Interactions*; Plenum: New York, 1980.
(37) Ohtaki, H.; Yamatera, H. *Structure and Dynamics of Solutions*; Elsevier: Amsterdam, 1992; p 15.

concentration of the hydrogen bonding solvent and salt can be varied independently.

Experimental Methods

Methanol (MeOH, absolute, EM Science, 500 mL) was dehydrated by refluxing over CaH_2 (5 g, Baker) for 2 h. The dried solvent was distilled under a dry N_2 atmosphere onto freshly activated 4 Å molecular sieves (Linde). The first 50 mL of the distillate were discarded and the next 300 mL were collected. *N*,*N*-Dimethylformamide (DMF, 99%, EM Science), *N*-methylformamide (NMF, 99%, Aldrich), and formamide (FA, 99%, EM Science) were dried by adding 5 g of BaO (Baker) to 500 mL of each solvent. Each mixture was allowed to sit for 12 h, then distilled over fresh BaO under reduced pressure onto 4 Å molecular sieves. Nitromethane (NM, 96%, Aldrich) was dried by the addition of 5 g of CaH_2 to 500 mL and allowed to sit for 24 h. The dried solvent was distilled under reduced pressure onto fresh CaH_2. All solvents were stored in dark glass bottles in a drybox under a nitrogen atmosphere.

Tetrabutylammonium thiocyanate (NBu_4SCN, >99%, Fluka) was dried under vacuum over P_2O_5 at 45 °C for 24 h. Tetrabutylammonium selenocyanide (NBu_4SeCN) was prepared from tetrabutylammonium chloride (98%, Aldrich) and potassium selenocyanide (98%, Aldrich). Potassium selenocyanide was dissolved in acetone and the solution was filtered to remove insoluble material. The potassium selenocyanide was recovered from the acetone solution through precipitation by ethyl ether. Tetrabutylammonium selenocyanide was prepared by mixing equimolar amounts of tetrabutylammonium chloride and potassium selenocyanide in acetone. The solution was filtered to remove the KCl precipitate and the solvent was removed from the filtrate to obtain NBu_4SeCN. The crude tetrabutylammonium selenocyanide was recrystalized in bis(2-ethoxy)ethane (Eastman), then dried in a vacuum oven at 45 °C for 24 h.

Solutions with known concentrations were prepared by weighing the solute on an analytical balance in a 5- or 25-mL volumetric flask and diluting with the appropriate solvent. All solution preparation was done in a drybox under a nitrogen atmosphere. Ternary solutions of the tetrabutylammonium salt and hydrogen bonding solvent in nitromethane were prepared from stock nitromethane solutions of the salt or the hydrogen bonding solvent. Aliquots (1, 2, 3, and 4 mL) of the salt or hydrogen bonding solvent solution were pipetted into 5-mL volumetric flasks so that the concentration of the salt and of the hydrogen bonding solvent could be varied independently.

Infrared spectra were recorded on a Nicolet 520P (Nicolet, Inc.) FTIR spectrometer. The 4800−900-cm^{-1} region was obtained at 1-cm^{-1} resolution using CaF_2 windows; the 4800−700-cm^{-1} region was obtained at 1-cm^{-1} resolution using Irtran-2 windows. The number of scans was varied from 200 to 10 000 depending on the absorptivity of the band studied. Teflon spacers were used to vary the path length of the cell, the pathlength value being determined by the fringe method.[38] Between each sample, the cell was flushed with 1−2 mL of the new sample to be studied and the spectrometer was purged with N_2 for 5 min prior to the collection of a new spectrum.

Multinuclear NMR spectra (^{14}N and ^{77}Se) were obtained on a VXR-500 FT-NMR spectrometer (Varian, Inc.). Each sample was placed in a 5-mm NMR tube with a coaxial insert containing an external reference and lock solvent. ^{14}N spectra were externally referenced to 1 M NBu_4NO_3 in $(CD_3)_2CO$ with respect to nitromethane (0.00 ppm). ^{77}Se spectra were externally referenced to 1 M diphenylselenocyanide in $(CD)_3CO$. The temperature probe in the spectrometer was calibrated by the known temperature dependence of the proton chemical shifts in methanol.[24]

Spectral envelopes were fitted to Gaussian/Lorenztian bandshapes[35] in order to determine the number of vibrational components and yield quantitative information about each component band. Sigma Plot (v. 4.14, Jandel Scientific, Inc.) was used to curve fit the infrared band envelopes. Spectral regions of interest, generally 100 cm^{-1}, were converted to ASCII files and imported as text files into Sigma Plot.

(38) Robinson, J. W. *Practical Handbook of Spectroscopy*; CRC Press: Boca Raton, 1991; p 508.

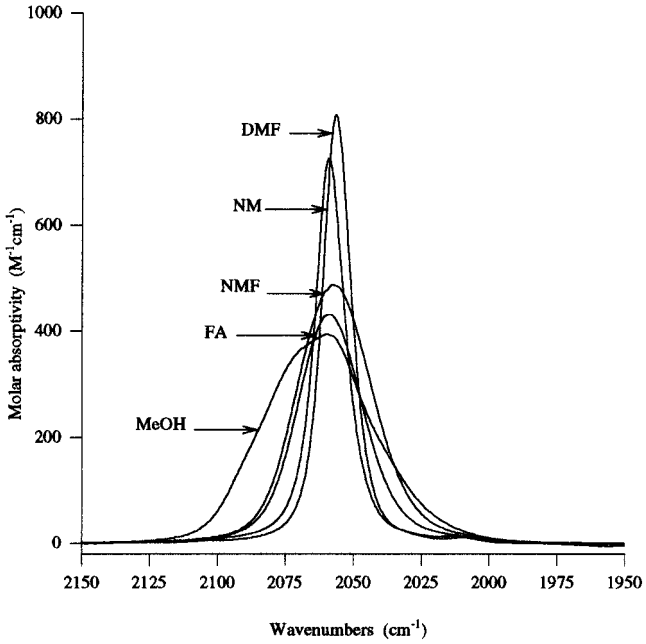

Figure 1. ν_{CN} stretch for ~0.25 M NBu_4SCN in DMF, NM, NMF, FA, and MeOH.

Table 1. Peak Position and Bandwidth for the ν_{CN} Stretch of ~0.25 M NBu_4SCN and ~0.1 M NBu_4SeCN in NM, DMF, NMF, FA, and MeOH

solvent system	ν_{CN} (cm^{-1})	$\Delta\nu_{1/2}$ (cm^{-1})
SCN^-		
NM	2059.5	13.5
DMF	2056.5	12.5
NMF	2057.8	34.0
FA	2059.5	27.5
MeOH	2060.0	40.5
$SeCN^-$		
NM	2068.0	12.0
DMF	2066.5	12.5
NMF	2067.5	28.0
FA	2068.0	24.0
MeOH	2076.5	46.0

Results and Discussion

The ν_{CN} stretching vibration of the SCN^- anion is sensitive to electrostatic interactions in solution. Hydrogen bonding significantly broadens the absorption and shifts the peak frequency of this mode compared to solutions of SCN^- in aprotic solvents, as shown in Figure 1 and summarized in Table 1. The bandshape of the spectral envelope, especially for methanol solutions, is complex and results from several overlapping component bands. Spectral enhancement techniques such Fourier self-deconvolution and curve fitting can be applied to obtain the underlying band structure, as shown in Figure 2. Closer inspection of the ν_{CN} mode for SCN^- in aprotic solvents shows that this mode is asymmetric and can be simulated by two bands, a "free" ν_{CN} vibration and a smaller band attributable to the $\nu_3 + \nu_2 - \nu_2$ (hot band) vibration about 7 cm^{-1} lower in energy. In the amide solvents, NMF and FA, the spectral envelope is found to consist of three bands; an additional band at higher energy is found in the methanol solution. The peak frequencies and widths of the component bands are given in Table 2. The ν_{CN} stretch for 0.025 M $SeCN^-$ in aprotic solvents is also asymmetric and is well modeled by incorporating a bending hot band about 7 cm^{-1} below that of the fundamental. In the protic solvents, NMF, FA, and MeOH, the ν_{CN} vibration of $SeCN^-$ is broader than in aprotic solvents (Table 1) and

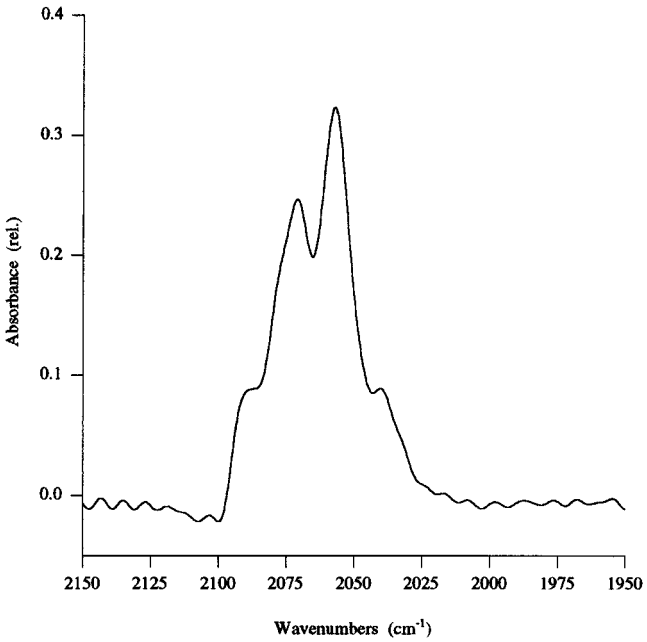

Figure 2. Fourier self-deconvolution of the ν_{CN} stretch for ~0.25 M NBu_4SCN in MeOH.

Table 2. Summary of the Deconvolved Parameters for the Component Bands in of the ν_{CN} Stretch for ~0.25 M NBu_4SCN in NM, DMF, NMF, FA, and MeOH and for ~0.1 M NBu_4SeCN in the Same Solvents

solvent system	ν_{CN} (cm^{-1})	$\Delta\nu_{1/2}$ (cm^{-1})
SCN^-		
NM[a]	2052.0 ± 0.1	12.4 ± 0.3
	2059.2 ± 0.1	12.2 ± 0.1
DMF[a]	2050.0 ± 0.1	12.3 ± 0.2
	2056.7 ± 0.1	11.8 ± 0.1
NMF	2048.0 ± 0.5	25.4 ± 0.2
	2058.2 ± 0.2	15.1 ± 0.8
	2067.5 ± 0.5	20.4 ± 0.2
FA	2050.1 ± 0.8	23.0 ± 1.2
	2057.8 ± 0.3	14.0 ± 1.8
	2065.3 ± 1.0	20.8 ± 1.0
MeOH	2043.9 ± 0.7	29.3 ± 0.3
	2057.5 ± 0.1	20.2 ± 2.0
	2072.8 ± 0.2	24.8 ± 2.0
	2090.9 ± 0.6	15.8 ± 1.0
$SeCN^-$		
NM[a]	2060.8 ± 0.1	12.1 ± 0.2
	2068.2 ± 0.1	11.1 ± 0.1
DMF[a]	2060.8 ± 0.2	14.1 ± 0.4
	2066.4 ± 0.1	12.0 ± 0.1
NMF	2054.1 ± 0.4	24.8 ± 0.2
	2076.7 ± 0.3	20.8 ± 0.2
	2068.0 ± 0.3	20.6 ± 0.4
FA	2051.9 ± 0.3	29.6 ± 0.4
	2066.8 ± 0.2	22.4 ± 0.2
	2073.5 ± 0.2	24.4 ± 0.8
MeOH	2058.9 ± 2.0	48.0 ± 10.
	2065.5 ± 0.7	25.1 ± 0.2
	2086.3 ± 0.7	28.9 ± 2.0

[a] Hot band included for aprotic solvents only.

consists of a composite of three bands;[39] the parameters for these components are also summarized in Table 2.

A clearer picture of the formation of anion−solvent adducts can be obtained by adding either the protic solvent or the chalcocyanate anion to a dilute solution of the other in a weakly solvating ("inert") solvent, such as nitromethane (NM), for which the donor number is low. Infrared studies of the C−H stretching modes for NM show that this solvent only weakly

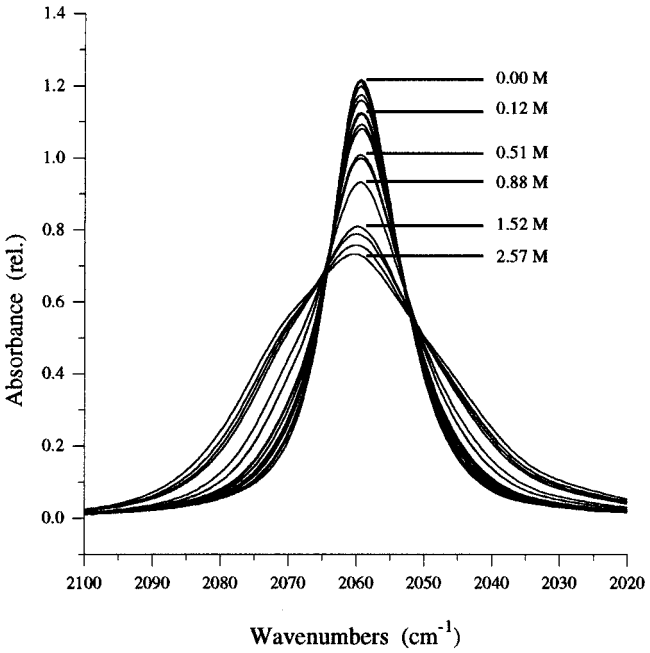

Figure 3. ν_{CN} stretch for ~0.1 M NBu_4SCN in NM with MeOH added.

solvates anions.[40] The low donicity of this solvent also precludes it from strongly interacting with electropositive species. Thus, the solvation of the thiocyanate anion by methanol can be followed by measuring the 2100−2000-cm^{-1} spectral envelope of ~0.1 M NBu_4SCN in NM as a function of added MeOH. When no methanol is present, the ν_{CN} stretch of SCN^- is a sharp absorption at 2059 cm^{-1}. As MeOH is added, the intensity of the 2059-cm^{-1} peak falls, with concomitant broadening of the spectral envelope, but virtually no change in the peak frequency. There are two isobestic points, observed above and below the peak maximum, which imply the formation of two thiocyanate−methanol complexes (Figure 3). In order to address the underlying composition of the spectral envelopes, the line shapes were Fourier self-deconvolved. The deconvolution procedure reveals that the absorbance of the central ν_{CN} component decreases as the concentration of MeOH increases. Concurrently, two new bands grow, at 2070 and 2047 cm^{-1}. Similar results are seen in the titration studies with NMF and FA.

Quantitative information can be obtained by fitting the absorption envelopes to Gaussian−Lorenztian sum components, which yields the absorbance, bandwidth, and peak position of each constituent band. The absorption curves in the methanol series can be well simulated with four components: at 2052 cm^{-1} for the hot band, at 2059 cm^{-1} for the free anion, at 2070 cm^{-1} for a methanol−thiocyanate complex, and at 2047 cm^{-1} for a second methanol−thiocyanate complex. The absorptivities of the fundamental constituents, plotted in Figure 4, are qualitatively similar to those obtained by the Fourier self-deconvolution of the experimental spectral envelopes. Similar titration experiments were performed by adding NMF and FA to solutions of 0.15 M NBu_4SCN in NM. Curve fitting and Fourier self-deconvolution of the 2100−2020-cm^{-1} spectral envelopes also show that the line shape in each case is a convolution of four bands (Table 3). The absorption envelope for $SeCN^-$ can also be well simulated by four bands: at 2062 cm^{-1} for the hot band, at 2069 cm^{-1} for the free anion, at 2078 cm^{-1} for a methanol−selenocyanide complex, and at 2061 cm^{-1} for a second methanol−thiocyanate complex (Table 4).

(39) Schultz, P. W. *Ph.D. Dissertation*, Michigan State University, 1995.

(40) Ramana, K.; Surjit, S. *J. Mol. Struct.* **1989**, *194*, 73.

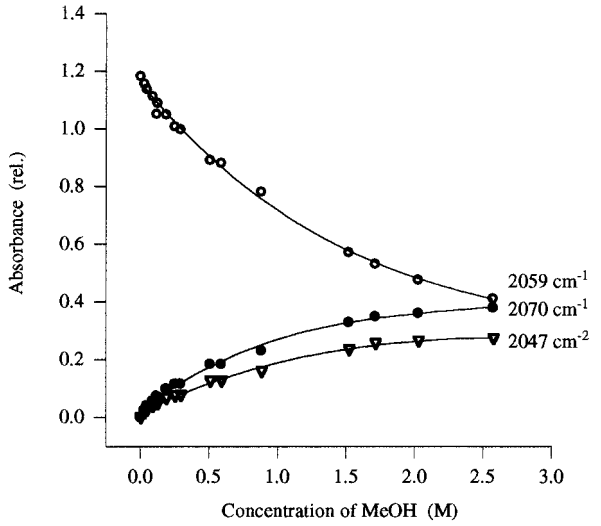

Figure 4. Absorptivities for component bands of the ν_{CN} mode of ~0.1 M NBu_4SCN in NM as a function of MeOH added.

Table 3. Summary of the Peak Positions and Bandwidths (cm^{-1}) from the Curve-Fitted Component Bands of the ν_{CN} and ν_{CS} Stretches of 0.15 M NBu_4SCN in NM with NMF, FA, or MeOH Added

solvent system	ν_{CN} peak position	$\nu_{1/2}$ fwhh	ν_{CS} peak position	ν_{CS} fwhh
NMF	2050.0 ± 1.0	17.4 ± 0.8	739.5 ± 0.6	11.4 ± 0.8
	2059.2 ± 0.2	12.2 ± 0.2	751.0 ± 0.4	10.3 ± 2.6
	2068.8 ± 1.4	13.2 ± 2.2		
FA	2050.7 ± 1.0	15.8 ± 2.8	739.8 ± 0.4	12.8 ± 1.2
	2059.2 ± 0.1	11.8 ± 0.3	751.4 ± 1.6	13.0 ± 1.6
	2067.2 ± 2.0	14.3 ± 1.8		
MeOH	2047.0 ± 1.0	20.4 ± 3.0	739.5 ± 0.3	11.4 ± 0.4
	2059.4 ± 0.1	12.8 ± 1.2	751.7 ± 0.8	14.5 ± 2.0
	2070.5 ± 0.4	13.2 ± 4.0		

Table 4. Summary of the Peak Positions and Bandwidths (cm^{-1}) from the Curve-Fitted Component Bands of the ν_{CN} Stretch of 0.025 M NBu_4SeCN in NM with MeOH Added

solvent system	ν_{CN} peak position	$\nu_{1/2}$ fwhh
MeOH	2060.7 ± 1.6	15.86 ± 3.60
	2068.8 ± 0.1	10.60 ± 1.04
	2077.5 ± 0.4	15.38 ± 1.68

Hydrogen bonding interactions with these anions perturb not only the frequencies of the stretching vibrations but also their absorptivity. The integrated absorptivity for the ν_{CN} stretch increases by 30% in the methanol titration series. Likewise, the integrated intensity for the ν_{CN} stretch in the NMF and FA titration series each increases by 13%. Experimental studies have shown that ionic and hydrogen bonding interactions to the nitrogen atom of SCN^- increase the absorptivity of the ν_{CN} stretch.[41−43] They are supported by our theoretical study, which predicts that electrostatic interactions to the nitrogen of SCN^- and $SeCN^-$ increase the molar absorptivity of the ν_{CN} mode in these anions.[14]

The 770−720-cm^{-1} spectral region contains the ν_{CS} mode and a vibration from the NBu_4^+ cation. In a 0.15 M NBu_4SCN solution in NM, this band is centered at 740 cm^{-1}. Addition of MeOH broadens the absorption and shifts the maximum of the envelope, with growth of a band at 752 cm^{-1}, as shown in Figure 5. This spectral envelope and similar spectra

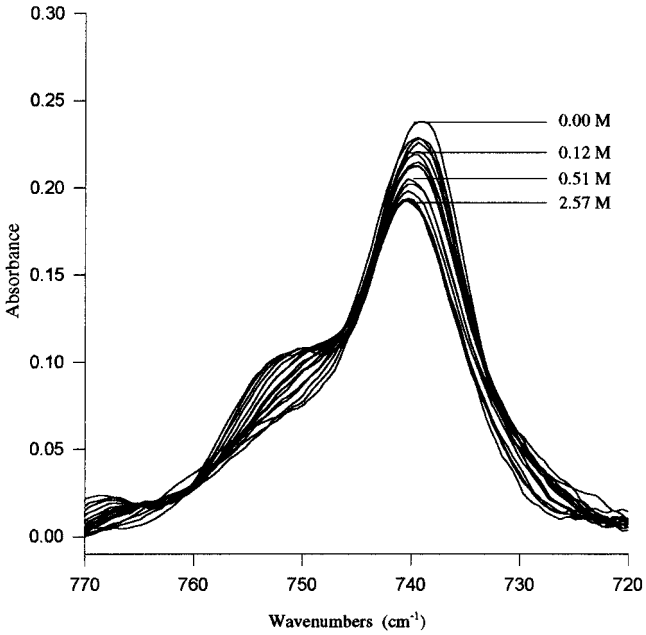

Figure 5. ν_{CS} stretch for ~0.1 M NBu_4SCN in NM as a function of MeOH added.

obtained from NMF or FA titrations can be simulated adequately by two Gaussian−Lorenztian sums (Table 3).

Assignments. The structure of the primary solvation sphere surrounding the thiocyanate anion in neat solutions of NBu_4SCN in MeOH, FA, and NMF can be understood by identifying the component bands of the two stretching modes. The concentration dependence of the infrared absorbances for the component bands in the titration studies, exemplified in Figures 3 and 5, shows clearly that the SCN^- anion is involved in two equilibria that have 1:1 stoichiometry. The most straightforward assignments are those for the unperturbed or "free" SCN^-; these bands occur at 2059 cm^{-1} for the ν_{CN} mode and 740 cm^{-1} for the ν_{CS} mode. Complexation along the molecular axis to either end of SCN^- leads to positive frequency shifts for the ν_{CN} mode.[6] These two types of interactions can be easily distinguished by the perturbations of the ν_{CS} mode. An electrostatic interaction to the nitrogen atom in SCN^- will blue shift this mode, whereas an electrostatic interaction to the sulfur will result in a red shift.[6,14] Clearly, there is no ν_{CS} component lower in energy than that for the "free" SCN^-, which implies that the 2070-cm^{-1} band must be due to a $SCN^-\cdots$HOMe complex. The red-shifted bands in the ν_{CN} mode of SCN^- have previously been assigned to complexes having nonaxial interactions to the nitrogen atoms,[18] where one or two solvent molecules are associated with the complex. The concentration dependence of the 2047-cm^{-1} band suggests that the stoichiometry of the complex is 1:1. Thus, the lower frequency band is attributed to a 1:1 complex with a nonaxial hydrogen bond to the nitrogen atom. Theoretical calculations support these assignments. They predict that hydrogen bonding to the nitrogen atom by hydrogen fluoride or water will increase the frequency of the stretching modes when the interaction is along the molecular axis.[14] On the other hand, a nonaxial hydrogen bonded complex will be characterized by a red-shift for the ν_{CN} stretch and a slight blue-shift in the ν_{CS} stretch.[44] Additional support for this unusual hydrogen bonded complex is derived from the crystal structure of $Na^+(12C4)_2$ $SCN^-\cdot$HOMe, where the C−N−O angle is 113°.[44] In the infrared spectrum of this solvate the ν_{CN} mode lies 12 cm^{-1} below that of the ν_{CN} stretch in $Na^+(12C4)_2SCN^-$.

(41) Kinnell, P. O.; Stranberg, R. *Acta Chem. Scand.* **1959**, *13*, 1607.
(42) Hart, G. W.; Hollenberg, J. L. *Spectrochim. Acta, Part A* **1969**, *34*, 367.
(43) Chabanel, M.; Bencheikh, A.; Puchalska, D. *J. Chem. Soc., Dalton Trans.* **1989**, 2193.
(44) Schultz, P. W.; Ward, D. L.; Popov, A. I.; Leroi, G. E. *J. Phys. Chem.* In press.

The same assignments can be made for the ν_{CN} components deconvolved from the spectra in the selenocyanide titration. The low-frequency band is attributed to a solvent adduct with a non-axial interaction to the nitrogen end of the anion and the high-frequency component to a complex having an axial interaction to the nitrogen atom.

The assignments from the titration experiments can be applied to the neat protic solutions. In the neat amide solutions, bands both above and below the "free" component at ~2058 cm^{-1}, which can be assigned to the "free" SCN^-, are found. They can be attributed to solvent interactions along the molecular axis of the anion and a nonaxial interaction, respectively. It should be noted that our experiments cannot differentiate between one and two nonlinear interactions, since the bands are so strongly overlapped. Similar structure is observed in methanol solutions. The band at 2058 cm^{-1} can be assigned to "free" SCN^-, the band at 2044 cm^{-1} to a non-axial interaction, and the 2073-cm^{-1} component to an axial interaction at the nitrogen end of the anion. The additional band at 2091 cm^{-1} is probably due to a MeOH···SCN^-···HOMe complex since a red-shifted component in the ν_{CS} mode is not observed. The component bands of the ν_{CN} envelope for $SeCN^-$ in NMF, FA, and MeOH can be attributed to free and hydrogen bonded complexes like those seen in SCN^-. A band attributable to a 1:2 solvate was not observed in any $SeCN^-$ solutions.

Thermodynamics. In addition to multiple associations of the thiocyanate or selenocyanide anions with the hydrogen bonding solvents, both the self-association of the hydrogen bonding solvent and ion pairing of the NBu_4SCN or NBu_4SeCN salts in nitromethane must be considered and possibly incorporated into the model for the solution equilibria. Previous investigations of the tetraalklyammonium salts in nitromethane have shown that ion pairing is negligible at 0.1 M.[45] Therefore, the results of our NMR and infrared measurements have been modeled by three equilibria: (a) the self-association of the hydrogen bonding solvent (limited to the dimerization) and (b) formation of two 1:1 anion−hydrogen bonding solvent adducts, as illustrated for thiocyanate and MeOH in eqs 1−3. Although these equilibrium expressions are written with the hydrogen bonding interaction at the nitrogen end of SCN^-, the determination of the equilibrium constants is independent of the site of the hydrogen bond. At the low concentrations of SCN^- and $SeCN^-$ employed in this work, the equilibrium constants can be written in terms of the concentrations of the species in the equilibria; the activity coefficients can be neglected.

$$SCN^- + MeOH \overset{K_1}{\rightleftharpoons} SCN^-\cdots HOMe \quad (1)$$

$$SCN^- + MeOH \overset{K_2}{\rightleftharpoons} SCN^-\cdots HOMe \text{ (nonaxial)} \quad (2)$$

$$2MeOH \overset{K_D}{\rightleftharpoons} (MeOH)_2 \quad (3)$$

Equation 4 gives the total concentration of SCN^- in terms of the concentration of the free SCN^- anion, $[SCN^-]_f$, the concentration of the first 1:1 complex, $[SCN^-\cdots HOMe]_1$, and the concentration of the second 1:1 complex $[SCN^-\cdots HOMe]_2$. Likewise, the total concentration of MeOH, $[MeOH]_T$, can be written in terms of the concentrations of free MeOH, $[MeOH]_f$, the two 1:1 complexes, and the methanol dimer, $[(MeOH)_2]$, according to eq 5.

$$[SCN^-]_T = [SCN^-]_f + [SCN^-\cdots HOMe]_1 + [SCN^-\cdots HOMe]_2 \quad (4)$$

$$[MeOH]_T = [MeOH]_f + [SCN^-\cdots HOMe]_1 + [SCN^-\cdots HOMe]_2 + 2[(MeOH)_2] \quad (5)$$

Substitution of equilibrium expressions for eqs 1−3 into eqs 4 and 5 and solution of the resulting equations simultaneously for $[SCN^-]_f$ yields a cubic expression in $[MeOH]_f$, eq 6. The

$$\{2K_D(K_1 + K_2)\}[MeOH]_f^3 + (K_1 + K_2 + 1)[MeOH]_f^2 + \{(K_1 + K_2)([SCN^-]_T - [MeOH]_T) + 1\}[MeOH]_f - [MeOH]_T = 0 \quad (6)$$

roots of eq 6 can be determined analytically, from which an expression for the concentration of free methanol can be derived in terms of the association constants, $K_1 + K_2$, and K_D. It should be noted that since K_1 cannot be separated from K_2, only the sum can be determined. An expression for $[SCN^-]_f$ can be written in terms of the association constants and the total MeOH and SCN^- concentrations by substituting expressions for K_1 and K_2 and the solution for eq 6 into eq 4.

The observed NMR chemical shift of either the ^{14}N or the ^{77}Se (for $SeCN^-$) resonance in these anions, δ_{obs}, is a population average of those for the free anion and both 1:1 complexes as shown in eq 7, where χ_{free} is the mole fraction and δ_{free} is the chemical shift of the free anion, χ_1 is the mole fraction of the first 1:1 complex and δ_1 is its chemical shift, and χ_2 is the mole fraction of the second 1:1 complex, which has the chemical shift δ_2. With the appropriate substitutions, eq 7 can be rewritten (exemplified for the SCN^-/MeOH system in eq 8) such that the observed chemical shift is a function of the association constants (K_1, K_2, and K_D), the free SCN^- concentration, the free MeOH concentration, and the limiting chemical shifts for the free SCN^- and the 1:1 complexes. Following substitution of the expressions for $[SCN^-]_f$ and $[MeOH]_f$, the values for the equilibrium constants, including K_D, can then be calculated by fitting eq 8 to the chemical shifts observed at different methanol concentrations. Again, individual association constants, K_1 and K_2, cannot be determined; the analysis yields only their sum or the parameter $K_1(\delta_1-\delta_2) + K_2(\delta_1-\delta_2)$. The derived values for the equilibrium constants are summarized in Table 5. The experimental data at several temperatures are illustrated by the SCN^-/MeOH titration in Figure 6.

$$\delta_{obs} = \chi_{free}\delta_{free} + \chi_1\delta_1 + \chi_2\delta_2 \quad (7)$$

$$\delta_{obs} = \{K_1(\delta_1-\delta_f) + K_2(\delta_2-\delta_f)\}[SCN^-]_f[MeOH]_f/[SCN^-]_T + \delta_{free} \quad (8)$$

The line width of the ^{14}N resonances can also be used to obtain association constants for these adducts. Under the condition of fast exchange between the free (f) and the bound (b) sites, and in the absence of exchange broadening, the spin−lattice relaxation time ($1/T_{1obs}$) is the population average of the relaxation times for the free ($1/T_{1f}$) and the bound ($1/T_{1b}$) species. For quadrupolar nuclei such as ^{14}N in asymmetric environments, the longitudinal relaxation rate is very fast and is the dominant relaxation pathway.[46] In such systems, the approximation $1/T_{1obs} = 1/T_{2obs}$ can be made, thereby relating the line width of the ^{14}N resonance to the association constants for the complex

(45) Hojo, M.; Miyauchi, Y.; Imai, Y. *Bull. Chem. Soc. Jpn.* **1990**, *63*, 3288.

(46) Abragam, A. *The Principles of Nuclear Magnetism*; Oxford University Press: New York, 1961.

Table 5. Association Constants, $(K_1 + K_2)$ and K_D, for the Formation of the Two 1:1 Complexes and Self-Association of the Protic Solvent, Determined by ^{14}N NMR Measurements for SCN^- Systems

solvent system	^{14}N chemical shift		^{14}N line width	
	$(K_1 + K_2)$	K_D	$(K_1 + K_2)$	K_D
MeOH				
25.0 °C	0.83 ± 0.01	0.10 ± 0.01	0.84 ± 0.03	0.10 ± 0.01
12.5 °C	1.05 ± 0.01	0.11 ± 0.01	0.95 ± 0.05	0.10 ± 0.01
0.0 °C	1.37 ± 0.01	0.13 ± 0.01	1.34 ± 0.05	0.14 ± 0.01
−12.5 °C	1.70 ± 0.02	0.15 ± 0.01	1.64 ± 0.09	0.15 ± 0.01
−25.0 °C	2.07 ± 0.02	0.17 ± 0.01	2.12 ± 0.07	0.14 ± 0.01
FA				
25.0 °C	0.76 ± 0.01	0.07 ± 0.01	0.74 ± 0.02	0.07 ± 0.01
12.5 °C	0.90 ± 0.01	0.07 ± 0.01	0.92 ± 0.05	0.08 ± 0.01
0.0 °C	1.05 ± 0.01	0.09 ± 0.01	1.01 ± 0.04	0.08 ± 0.01
−12.5 °C	1.27 ± 0.01	0.10 ± 0.01	1.25 ± 0.05	0.09 ± 0.01
−25.0 °C	1.46 ± 0.02	0.11 ± 0.01	1.43 ± 0.05	0.10 ± 0.01
NMF				
25.0 °C	0.71 ± 0.01	0.05 ± 0.01	0.70 ± 0.04	0.04 ± 0.01
12.5 °C	0.85 ± 0.01	0.06 ± 0.01	0.85 ± 0.05	0.05 ± 0.01
0.0 °C	0.94 ± 0.01	0.07 ± 0.01	0.94 ± 0.06	0.06 ± 0.01
−12.5 °C	1.00 ± 0.01	0.07 ± 0.01	0.99 ± 0.03	0.06 ± 0.01
−25.0 °C	1.18 ± 0.03	0.09 ± 0.01	1.22 ± 0.09	0.07 ± 0.01

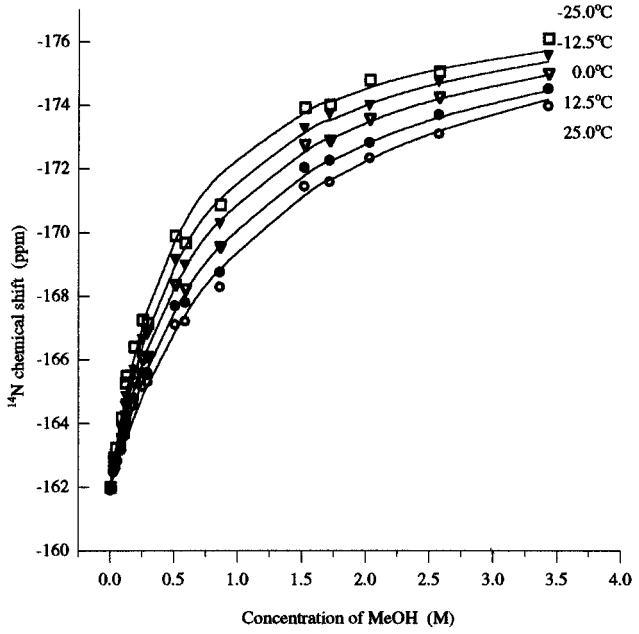

Figure 6. ^{14}N NMR chemical shift for ∼0.1 M NBu_4SCN in NM as a function of MeOH concentration and temperature.

formation, since the line width of an NMR resonance ($\Delta\nu$) is proportional to the reciprocal of the transverse relaxation rate, eq 9. Again, the relationships for $[SCN^-]_f$ and $[MeOH]_f$ discussed previously can be substituted for the concentrations of free SCN^- and MeOH. Figure 7 shows the ^{14}N line width dependence on temperature and MeOH concentration for ∼0.1 M SCN^- in NM. The association constant sums and the dimerization constants determined from the line width analysis are also collected in Table 5. The agreement between the values determined by the two methods is excellent.

$$\Delta\nu_{1/2} = \frac{2}{\pi T_2} \approx \frac{2}{\pi}\left(\frac{\chi_f}{T_{1f}} + \frac{\chi_b}{T_{1b}}\right) = \frac{2[SCN^-]_f[MeOH]_f}{\pi[MeOH]_T}\left(\frac{1}{T_{1b}} - \frac{1}{T_{1f}}\right) + \frac{2}{\pi T_{1f}} \quad (9)$$

Similarly, the ^{77}Se and ^{14}N resonances in NBu_4SeCN are sensititive to electrostatic interactions and the concentration

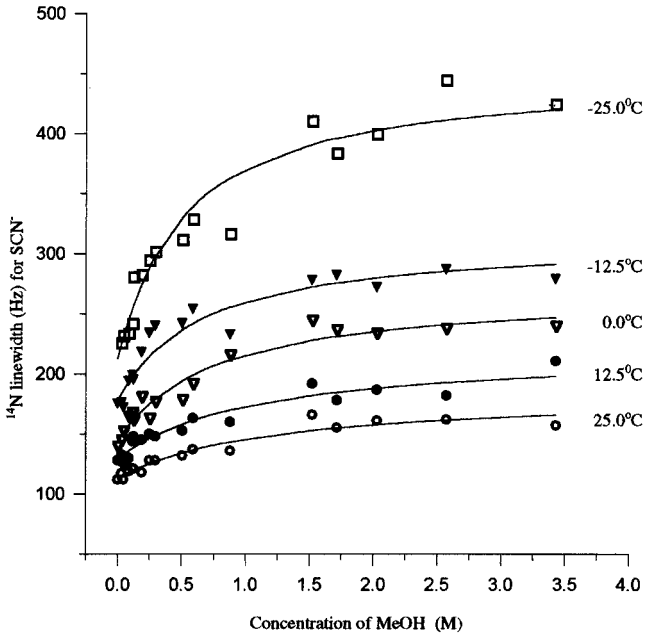

Figure 7. ^{14}N line width of ∼0.1 M NBu_4SCN in NM as a function of MeOH concentration and temperature.

dependences can be fitted to the models described earlier. At room temperature, the $(K_1 + K_2)$ parameter from the ^{77}Se chemical shift is 0.68 ± 0.06 M^{-1}, whereas the value is 0.69 ± 0.01 M^{-1} from the ^{14}N resonance. Similar to the ^{14}N experiments for SCN^-, the line width of the nitrogen resonance for $SeCN^-$ increases as a function of MeOH added; however, the line width for the ^{77}Se resonance of $SeCN^-$ remains constant throughout the titration series. This observation confirms that the line broadening in the ^{14}N resonances for $SeCN^-$ does not result from exchange broadening.

The formation constants for the hydrogen bonded complexes can also be determined in a number of ways from the concentration dependence of the infrared band absorptivities. The absorptivity of the 2059-cm^{-1} component can be related to $[SCN^-]_f$ and $[MeOH]_f$ as shown in eq 10, where ϵ_{2059} is the molar absorptivity and l is the path length of the infrared cell. Upon substitution for $[MeOH]_f$, the absorbance of the 2059-cm^{-1} component becomes a function of the molar absorptivity, path length, equilibrium constants, and the total concentrations of SCN^- and MeOH. The fitting of eq 10 to the absorbance of the ν_{2059} band provides the formation constants of the solvated complexes and the self-association constant for the solvent. Likewise, the absorbance of the blue-shifted and red-shifed component bands in the methanol titration can also be related to the total SCN^- and MeOH concentrations. The integrated intensity of the ν_{CN} mode provides a fourth method for obtaining the association constants, since the molar absorptivities of the complexes are larger than that for the unperturbed anion. The integrated absorptivity (A) is the sum of all the component band absorbances. With the appropriate subsitutions, the integrated

$$A_{2059} = \epsilon_{2059} l [SCN^-]_f = \frac{\epsilon_{2059} l [SCN^-]_T}{1 + (K_1 + K_2)[MeOH]_f} \quad (10)$$

absorptivity (A) can be written so that it is a function of the total concentrations of SCN^- and MeOH by substituting the relationship for $[MeOH]_f$ into eq 11. It should be noted that the inclusion of the second 1:1 hydrogen bonding equilibrium cannot be mathematically distinguished from a single 1:1 equilibrium, since the concentration dependencies will be the same. The $(K_1 + K_2)$ parameter obtained by fitting this model

Table 6. Association Constants ($K_1 + K_2$) and K_D, of SCN^- with MeOH, FA, and NMF from the Stretching Modes of SCN^-

solvent system	A_{2058}	$A_{\text{blue shift}}$	$A_{\text{red shift}}$	integrated absorptivity	A_{740}
MeOH					
$K_1 + K_2$	0.86 ± 0.02	0.86 ± 0.01	0.86 ± 0.01	0.83 ± 0.01	0.82 ± 0.04
K_D	$0.09 \pm 0..01$	0.10 ± 0.01	0.10 ± 0.01	0.09 ± 0.01	0.10 ± 0.01
FA					
$K_1 + K_2$	0.71 ± 0.01	0.70 ± 0.01	0.72 ± 0.01	0.72 ± 0.02	0.68 ± 0.09
K_D	0.06 ± 0.01	0.06 ± 0.01	0.06 ± 0.01	0.07 ± 0.01	0.06 ± 0.01
NMF					
$K_1 + K_2$	0.67 ± 0.01	0.62 ± 0.01	0.71 ± 0.01	0.71 ± 0.02	0.67 ± 0.06
K_D	0.06 ± 0.01	0.05 ± 0.01	0.05 ± 0.01	0.05 ± 0.01	0.05 ± 0.01

Table 7. Thermodynamic Parameters for the Association of SCN^- with MeOH, FA, and NMF from the NMR Measurements

solvent system	^{14}N chemical shift $\Delta H_{1+2}°$ (kJ/mol)	$\Delta S_{1+2}°$ (J mol^{-1} K^{-1})	^{14}N linewidth $\Delta H_{1+2}°$ (kJ/mol)	$\Delta S_{1+2}°$ (J mol^{-1} K^{-1})
MeOH	-11.4 ± 0.7	-40 ± 3	-11.8 ± 0.8	-41 ± 3
FA	-8.2 ± 0.3	-30 ± 1	-8.0 ± 0.6	-29 ± 2
NMF	-5.8 ± 0.7	-22 ± 2	-6.2 ± 0.8	-24 ± 3

to the experimental data provides additional confidence that the ν_{CN} spectral envelope is correctly simulated, since the model for the integrated absorptivity makes few assumptions about the equilibria involved in the ν_{CN} spectral envelope. If the ν_{CN} mode is simulated with only two Gaussian/Lorenztian bands, the association constant for the 1:1 complex calculated is substantially smaller than the $K_1 + K_2$ value determined by NMR. The results for the interaction of SCN^- with all three protic solvents are collected in Table 6.

$$A = \frac{l\,[SCN^-]_T}{1 + (K_1 + K_2)[MeOH]_f}(\epsilon_{free} + (K_1\epsilon_1 + K_2\epsilon_2)[MeOH]_f) \quad (11)$$

The ν_{CS} mode, in the titration series, was found to be a composite of two bands. The concentration dependence of these component bands can be fit by several models. The model that best fits the experimental data and is consistent with previous results assumes that the 740-cm^{-1} component is a composite band with contributions from the "free" SCN^- and one of the solvated complexes and that the 751-cm^{-1} component is the sum of a NBu_4^+ absorption and the other solvate complex. The absorbance at 740 cm^{-1} can be related to the total concentrations of SCN^- and MeOH, eq 12. The association constants calculated from the concentration dependence of the absorbance for this mode are in excellent agreement with those obtained for the ν_{CN} mode; see the last column of Table 6.

$$A_{740} = \epsilon_{free} l\,[SCN^-]_f + \epsilon_2 l\,[SCN^-\cdots HOMe]2 = \frac{l\,[SCN^-]_T}{1 + (K_1 + K_2)[MeOH]_T}(\epsilon_{free} + \epsilon_2 K_2[MeOH]_f) \quad (12)$$

Even though K_1 and K_2 cannot be separated in the NMR experiment, it was found that the temperature dependence of their sum fits the usual Gibb's free energy relationship. The computed enthalpy and entropy values (Table 7) are a convolution of the two equilibria that they represent. Despite the difficulty in interpreting the meaning and significance of these parameters, they are fairly similar to results we obtained for complexes of the cyanate anion with these protic solvents.[35] Here the ΔS_{1+2} values are larger than those for the cyanate association, whereas the enthalpy values for the thiocyanate complexes are smaller than those for the cyanate complexes.

Conclusions

The interactions of the thiocyanate and selenocyanide anions with the protic solvents MeOH, FA, and NMF are weak. Their strength is an order of magnitude weaker than the analogous solvation of the cyanate anion by these protic solvents,[35] which makes them difficult to study. In this work, we have investigated SCN^- and $SeCN^-$ solvates by a number of infrared, NMR and computational techniques in order to obtain an understanding of the structure of the primary solvation sphere. The concentration dependence of the integrated intensity for the ν_{CN} mode, the ^{14}N chemical shift, and the ^{14}N line width all fit a 1:1 equilibrium model. It should be noted that these models do not discriminate between two 1:1 equilibria and a single 1:1 equilibrium. The deconvolution procedures applied to the infrared spectral envelopes are not without ambiguity. For example, the ν_{CN} mode in the SCN^-/methanol titration experiments could have been fit by only three bands (the hot band, the "free" SCN^-, and a single SCN^-/MeOH complex) instead of four. However, the parameters from this procedure are not self-consistent; the peak positions and band widths of the component bands are not constant. Other authors have used more than four components to fit ν_{CN} of SCN^- in methanol.[18] Although four bands simulate this spectral envelope with insignificant residuals, a larger number of bands could be convolved in this line shape. The ν_{CS} stretch, which is very sensitive to electrostatic interaction, is more diagnostic for the number of vibrational components; this mode precludes a large number of vibrational components. If only a single 1:1 equilibrium model is utilized to deconvolve the stretching modes, the association constants are not in agreement with those obtained from the integrated absorbance, the ^{14}N chemical shift, and the ^{14}N line width data. We believe that we have correctly determined the presence of two 1:1 anion−solvate equilibria in our titration experiments from the harmony found among the results obtained by the disparate techniques.

The SCN^- and $SeCN^-$ anions are much less solvated than OCN^-. Whereas in MeOH, FA, and NMF solutions the OCN^- anion is associated with approximately 2 solvent molecules, a significant proportion of the SCN^- and $SeCN^-$ anions are not hydrogen bonded (i.e. "free") in neat solutions of these solvents. The titration studies show that the enthalpy of complex formation is smaller and the entropy of complex formation is larger for SCN^- and $SeCN^-$ solvation, as compared to OCN^-. A possible explanation is provided by the molecular electrostatic potential. *Ab initio* studies of these anions show that the cyanate anion has a more negative electrostatic potential off the nitrogen atom than is calculated for SCN^- and $SeCN^-$.[14] The smaller

electrostatic potential for SCN^- and $SeCN^-$ results in a smaller hydrogen bond enthalpy of formation. Although the net charge on all three anions is -1, the distribution of this charge is also important in how they order or structure the solvent molecules surrounding them. The smaller electrostatic potentials for SCN^- and $SeCN^-$ order the nitromethane molecules surrounding them less well than does OCN^-. Thus upon formation of a hydrogen bond with SCN^- or $SeCN^-$, fewer solvent molecules will be released, thereby resulting in a more negative entropy than for OCN^- complexation. Additional evidence is provided by the interactions at the chalcogen atom of OCN^-, SCN^-, and $SeCN^-$, for which the predicted electrostatic potential decreases in the same order.[14] In methanol solutions, a significant proportion of the cyanate anion is hydrogen bonded at the oxygen end, yet only a small percentage of the SCN^- is hydrogen bonded at the sulfur end and no detectable hydrogen bonding is observed at the selenium atom in $SeCN^-$/MeOH solutions.

JA960882V